The Detection of Esophagitis by Using Back Propagation Network Algorithm

Kwang-wook Seo, Byeong-ro Min, Dae-weon Lee*

Department of Bio-Mechartronic Engineering, SungKyunKwan University Suwon, Kyunggi-do 440-746, Korea

The results of this study suggest the use of a Back Propagation Network (BPN) algorithm for the detection of esophageal erosions or abnormalities — which are the important signs of esophagitis — in the analysis of the color and textural aspects of clinical images obtained by endoscopy. The authors have investigated the optimization of the learning condition by the number of neurons in the hidden layer within the structure of the neural network. By optimizing learning parameters, we learned and have validated esophageal erosion images and/or ulcers functioning as the critical diagnostic criteria for esophagitis and associated abnormalities. Validation was established by using twenty clinical images. The success rates for detection of esophagitis during calibration and during validation were 97.91% and 96.83%, respectively.

Key Words : Back Propagation Network, Endoscopy, Esophagitis, Texture

1. Introduction

The medical condition of a clinical disease or morphologic alteration involving the esophagus develops, as gastric acids or contents flow backwards to the esophagus, is termed Gastro Esophageal Reflux Disease (GERD). More broadly, this term indicates esophagitis and all esophageal complication (s) and diseases including this condition (Yoon et al., 2001).

Patients with GERD are increasingly diagnosed as a result of the world-wide-spread of Western eating habits. Korea is a nation included in this tendency towards Western eating habits which also frequently lead to obesity (Na et al., 1994).

Currently, endoscopy is a technique often used to determine the presence and size of erosions associated with GERD. Endoscopy is performed directly and with visualization by a physician. The endoscopic technique, however, can be restricted by the difficulty in detecting minor lesions given the limitations of human vision (Paul Fockens, 2002). Thus, the diagnosis of an esophageal abnormality at an early phase may not be possible (Krishnan and Yang, 1998).

Several studies have been suggested with the aim of detecting any esophageal erosions or abnormalities associated with GERD. Zheng et al. (2001) suggested that since many environmental factors that affect a human lesion are highly variable, it is very difficult to accurately detect abnormalities using a single evaluative technique. with a more effective analytic approach, when feasible, would be to apply multiple techniques (Zheng et al., 2001). In addition, Seo and colleagues (2004) have been able to detect abnormalities by segmenting an endoscopic film picture, extracting significant images from the color and texture parameters obtained from each segmented image, and thereafter conducting discriminant analyses.

In this study, endoscopic imaging of the gastroesophageal region was segmented into fixed

* Corresponding Author,
E-mail : daeweon@skku.edu
TEL : +82-31-290-7826; **FAX** : +82-31-290-7886
Department of Bio-Mechartronic Engineering, SungKyunKwan University Suwon, Kyunggi-do 440-746, Korea. (Manuscript **Received** January 31, 2006; **Revised** August 17, 2006)

sizes, and the BPN (Back Propagation Network) algorithm was applied yielding parameters of the images that support and that verify the technique for the detection of abnormalities.

2. Learning Design

2.1 BPN Algorithm

The BPN algorithm is a learning method involving output-layer error signals to change the connection weight between the hidden layer and the output layer and propagating output-layer error signals back to the hidden layer to change the connection weight between the input layer and the hidden layer.

The network consists of input-layer vector (x), hiddenlayer output vector (z) and output-layer output vector (y).

In addition, the connection weights between the input layer and the hidden layer and between the hidden layer and the output layer corresponding to v and w, respectively are expressed in the form of matrix.

In the learning method of BPN algorithm, s pairs of learning patterns (x_1, d_1), (x_2, d_2), $\cdots$, (x_s, d_s) are selected. Connection weights v and w are initialized into an arbitrary small value, setting an appropriate learning rate. The pairs of learning patterns are input in sequence and the connection weights are changed. Using a sigmoid function, the activation function for modifying connection weights enables the calculation of a weighted sum NET_z and output z in the hidden layer, a weighted sum NET_y and a final output y in the output layer. By comparing the target value d and the final output y, square error E was obtained (Eq. (1)).

$$E=\frac{1}{2}(d-y)^2 \tag{1}$$

As given in Eq. (2), the output-layer error signal δ_y and the error signal propagating to the hidden layer δ_z were calculated.

$$\delta_y=\frac{1}{2}(d-y)\,(1-y^2) \tag{2}$$

$$\delta_z=f\,(NET_z)\sum_{i=0}^{m}\delta_y w=\frac{1}{2}(1-z^2)\,\delta_y w \tag{3}$$

At any learning phase k, a variation in the connection weight between the hidden layer and the output layer Δw^k and a variation in the connection weight between the input layer and the hidden layer Δy^k were calculated by means of Eq. (4). At the learning phase $k+1$, the connection weight between the hidden layer and the output layer w^{k+1}, and the connection weight between the input layer v^{k+1} and the hidden layer is expressed by means of Eq. (5).

$$\Delta w^k=\alpha\delta_y z,\ \Delta v^k=\alpha\delta_z x \tag{4}$$

$$w^{k+1}=w^k+\Delta w^k,\ v^{k+1}=v^k+\Delta v^k \tag{5}$$

Connection weights were changed in the manner of repeating input of pairs of the learning patterns ; in the case that error E was smaller than a certain range $E_{\max}$, the learning was terminated.

2.2 Learning input pattern

The learning input pattern was composed of a total of twenty input elements (Karkanis et al., 2000). To detect GERD-associated erosions and ulcers with image processing, an input pattern using eight (8) color parameters and twelve (12) texture parameters which are characteristic of the image.

Among the eight color parameters used in the image processing field, they included R (Red), G (Green) and B (Blue) values of the RGB color model, H (Hue) and Gray values of the HSI model, and L (Lightness), a and b values of the Lab model (Tjoa and Krishnan, 2001). The H, L, a and b values, were those obtained from the formula using the R, G and B values of each pixel.

For texture parameters available for visualizing the relative distribution of colors against the respective pixels within an image, a total of twelve parameters including seven of GLCM (Grey Level Co-occurrence Matrices), one by vector dispersion, and four by surface curvature were used (Parker, 1997 ; Wang and Krishnan, 2001).

2.3 Learning design parameters

If incorrectly set, the initial connection weight may lead to the local minimum of error in learn-

ing, error divergence and delayed learning time. In this study, the connection weights between the hidden layer and the output layer were applied as one of values ranging from -0.5 to $+0.5$. The connection weight between the input layer and the hidden layer is as shown in Eq. (6) (Nguyen and Widrow, 2001).

$$v^{new}=\frac{\beta v_{old}}{\| v_{old} \|} \qquad (\beta=0.7\sqrt[n]{p}) \qquad (6)$$

where, n is the Number of input layer units and p is Number of hidden layer units.

The hidden layer was set to a single layer because it does not involve high efficiency in learning even though it has multiple-layer configuration. As the number of neurons in the hidden layer has an important influence upon learning, the optimization method to determine the number of neurons in the hidden layer is required. Accordingly, in this study, the number of neurons in the hidden layer was increased from two and the optimal number of those were set through repeated experiments.

The learning rate ranges spanned 0.0001 to 10; initially, an error signal by any error between the target value and the output value is calculated and then the connection weight is established. As smaller learning rates lead to slower learning speeds, and whereas higher learning rates result in larger error oscillations, the learning rate was seen to vary with various situations. Furthermore, to generate the next connection, Δv and Δw corresponding to gains in the existing connection weights v and w, respectively, were added to the existing weights. Additionally, the learning condition was improved by the operation with momentum. Table 1 indicates the learning parameters.

Table 1 Learning Parameters

Learning Parameters	Value
Number of Image Data Sets	10
Number of Input Data Units	20
Number of Total Data	26010 (2601×10) Locals
Number of Target Data Units	1 (N or A)
Number of Hidden-layer Units	2~12
Learning rate	0.1
Momentum Constant	0.9
Maximum System Error	0.005

3. Materials and Methods

3.1 Materials

Digital endoscopic images with a resolution of 256×256 were used for detecting abnormalities. These images were obtained from clinical trials at St. Mary's Hospital, the Catholic University of Korea, city, Korea. The number of the images to be used was set at 20 in total; for the algorithm calibration, two images of normal sites and eight images of abnormal sites were used. Similarly, for the algorithm validation as per the calibration, two images of normal sites and eight images of abnormal sites were used.

Even though the image has abnormal sites, every abnormal image includes both abnormal parts and normal parts. Therefore, the image of abnormal sites was used more than that of normal sites.

To acquire the image parameters and to learn the BPN, a desktop computer equipped with 2.4 GHz Pentium IV CPU was used. The software program used was Microsoft Visual C++ 6.0 where the GUI (Graphic User Interface) was

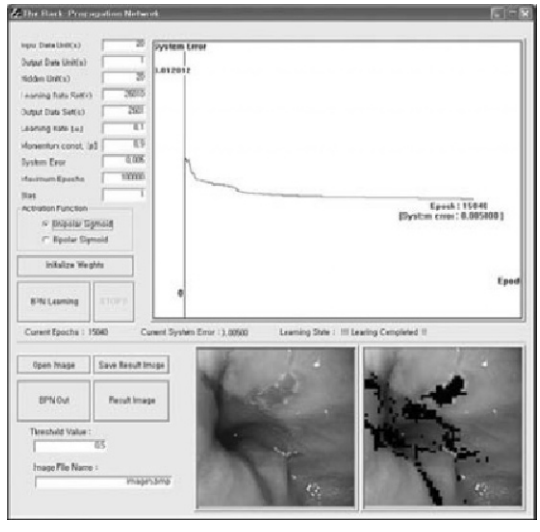

Fig. 1 View of main program

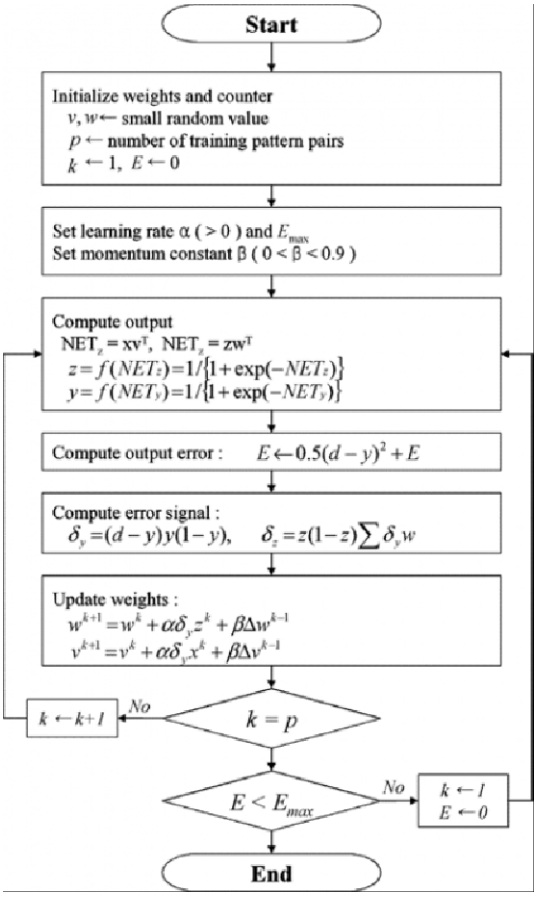

Fig. 2 Flow chart of the BPN algorithm

available for additional programming. Fig. 1 shows the prepared program which consists of image processing units and enables a comparison of any BPN learning components and the resulting image as a result of learning. Fig. 2 shows a flow chart where the BPN algorithm operates within the program.

3.2 Methods

The experimental phases of this study were divided into calibration and validation, and the abnormalities were subsequently detected with image processing. Calibration included segmenting the images obtained by endoscopy, calculating image parameters in the segmented local area, and establishment of connection weights through learning the BPN algorithm after selecting optimal learning parameters. The boundary values for discrimination the final output neuron were optimized by a trial-and-error method. During the validation phase, the abnormality detection process was validated by means of the algorithm learned by the BPN based upon the resultant connection weights.

3.2.1 Calibration

1) Image Segmentation

The images obtained in preprocessing for establishing image processing parameters from the experimental images should be segmented into the units of local regions and in this regard the image with a 256×256 resolution was subdivided into smaller local areas measuring 5×5. Through subdivision into the smaller local areas (51×51), 2601 were created in total. From these local areas, 20 image processing parameters including eight color parameters and twelve texture parameters, could be obtained.

2) Optimization of Learning Parameters

The number of neurons in the hidden layer leading to the optimal learning was created by a trial-and-error method, that performed learning while gradually increasing the number within the range of 2 to 22. In addition, when output values were determined through the established algorithm by the final learning parameters, the boundary value to separate preset target normal conditions from abnormal conditions was optimized. To divide the output values into the target values (0.1 and 0.9), the correlation between the boundary value and the success rate was subjected to nonlinear curve fitting in the equation of the n^{th} degree, as given in Eq. (7).

$$f(x) = a_0 + a_1 x + a_2 x^2 + \cdots + a_n x^n \qquad (7)$$

In Eq. (7), x is equal to boundary value, $f(x)$ to the success rate, and $a_0, a_1, a_2, \cdots, a_n$ to the n^{th} coefficient of $f(x)$.

3.2.2 Validation

To screen normality's and abnormalities through BPN from the connection weights obtained by learning, once an image to be validated was input, segmentation into local areas and operations with

image parameters were performed. Following operations, output values were obtained through the connection weights among neurons which were previously determined regarding their respective parameters during calibration. To decide whether a certain local area was normal or abnormal as the optimal boundary value, a new program had to be developed and validated.

4. Results and Discussion

4.1 Calibration

After setting the boundary values of the outcome values by learning to a level of 0.5, repeated learning experiments were implemented by gradually increasing the number of neurons in the hidden layer within the range from 2 to 22. The resulting success rates for normality detection and for abnormality detection were compared to the number of neurons in the hidden layer. When the number of neurons in the hidden layer was equal to 20, the success rates for normality detection and for abnormality detection were determined to be 98.91% and 74.55%, respectively. The entire success rate for detection was 97.80% and indicated the optimal condition had been reached. Table 2 shows the success rates for detection, by the number of neurons in the hidden layer. The total number of the local areas used in learning was 26,010, and of them, 24,935 appeared normal and 1,075 seemed abnormal.

To determine an output pattern, a regression curve of the boundary value separating normality's from abnormalities, and the success rates for detection were subject to curve fitting from the 2^{nd} to 10^{th} equations. The highest correlation

Table 2 Success rate by number of hidden layer neuron (Threshold value : 0.5)

Hidden Neuron	Successful Locals	Success Rate of All Locals (%)	Successful Normal Locals	Success Rate of Normal Locals (%)	Successful Abnormal Locals	Success Rate of Abnormal Locals (%)
2	25432	97.78	24732	99.19	699	65.03
3	25258	97.11	24595	98.64	663	61.68
4	25423	97.74	24752	99.27	671	62.38
5	25432	97.78	24732	99.19	699	65.03
6	25388	97.61	24732	99.19	656	60.98
7	25363	97.51	24649	98.85	714	66.43
8	25383	97.59	24731	99.18	653	60.70
9	25392	97.62	24696	99.04	696	64.76
10	25449	97.84	24783	99.39	666	61.96
11	25423	97.74	24786	99.40	637	59.30
12	25460	97.88	24774	99.36	686	63.78
13	25427	97.76	24742	99.23	684	63.64
14	25446	97.83	24819	99.54	627	58.32
15	25315	97.33	24567	98.52	749	69.65
16	25329	97.38	24630	98.78	699	65.03
17	25237	97.03	24567	98.52	671	62.38
18	25412	97.70	24702	99.07	710	66.01
19	25457	97.87	24767	99.32	690	64.20
20	25465	97.91	24664	98.91	801	74.55
21	25229	97.00	24511	98.30	717	66.71
22	25459	97.88	24732	99.19	726	67.55

was revealed in the 7th equation curve, as given in Table 3. The resulting regression curve appears as Eq. (8).

$$f(x) = -1.6862 + 35.67x - 201.94x^2 + 619.86x^3 - 1109.89x^4 + 1159.17x^5 - 654.90x^6 + 154.71x^7 \quad (8)$$

The optimal boundary value was shown in the position of $f'(x)$ which is the linear derived function of the regression curve, and the maximum was shown at. Thus, the boundary value was determined as 0.55. Fig. 3 is the graph derived from Eq. (8) showing the success rates of detection according to boundary values.

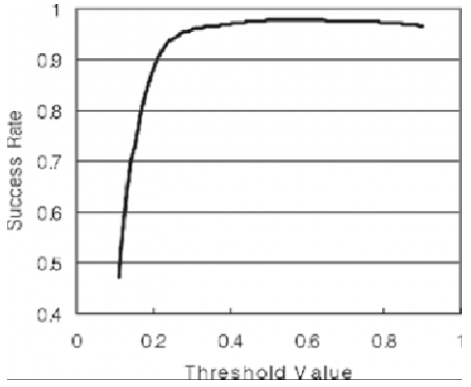

Fig. 3 The relationship between success rate and threshold value

4.2 Validation

With the connection weight and boundary values established based upon the above-mentioned results of calibration, 10 images to be validated were processed. The results of the respective local areas were intentionally calculated within the range of 0 to 1, and in the case of a result smaller than the boundary value 0.55, it was arbitrarily recognized as an abnormal region (A). In the case of a result larger than the boundary value 0.55, it was recognized as a normal region (N). Table 4 shows the results of validation for the ten images and demonstrates the result of distinguishing abnormal local from normal local areas of the images.

Of the entire set of ten endoscopy images, including eight with esophagitis, No. 1 (99.7%) and 4 (99.4%) showed the highest success rates

Table 3 Mean Error and R2 of nth (n=2,3,⋯,10) curve fitting equation

n^{th} eq.	2	3	4	5	6	7	8	9	10
R^2	0.8124	0.9137	0.9585	0.9743	0.9783	0.9886	0.9789	0.9805	0.8965
Mean Err.	0.0409	0.0288	0.0186	0.013	0.0094	0.008	0.0091	0.0104	0.04

Table 4 Success rate of validation images

Image No.	Successful Locals	Success Rate of All Locals (%)	Normal Locals	Successful Normal Locals	Success Rate of Normal Locals (%)	Abnormal Locals	Successful Abnormal Locals	Success Rate of Abnormal Locals (%)
1	2593	99.69	2565	2561	99.84	36	32	88.89
2	2343	90.08	2497	2273	91.03	104	70	67.31
3	2400	92.27	2306	2137	92.67	295	263	89.15
4	2585	99.38	2562	2552	99.61	39	33	84.61
5	2519	96.85	2499	2435	97.41	102	84	82.35
6	2538	97.58	2491	2452	98.43	110	86	78.18
7	2486	95.58	2347	2072	88.28	492	414	84.15
8	2537	97.54	2468	2439	98.82	133	98	73.68
9	2595	99.77	2601	2595	99.77	0	—	—
10	2589	99.54	2601	2589	99.54	0	—	—

for detection, with a mean success rate of 96.9%. Based on these results, it was considered that this method is capable of detecting minor lesions through the BPN algorithm and to aid the diagnoses of such esophageal abnormalities as esophagitis using digital endoscopic imaging. Table 5 shows the general result of validation. The detection rates of normality and abnormality were determined to be 96.54% and 81.04%, respectively, and as a result the false positive for normality and true negative for abnormality rates were 3.46% and 18.96%, respectively. Fig. 4 shows the result images after input images and image processing that were performed in this study and in summary suggests that abnormalities can be accurately detected.

Table 5 Result of validation

Output	Normal	Abnormal
Normal	95.54%	3.46%
Abnormal	18.96%	81.04%

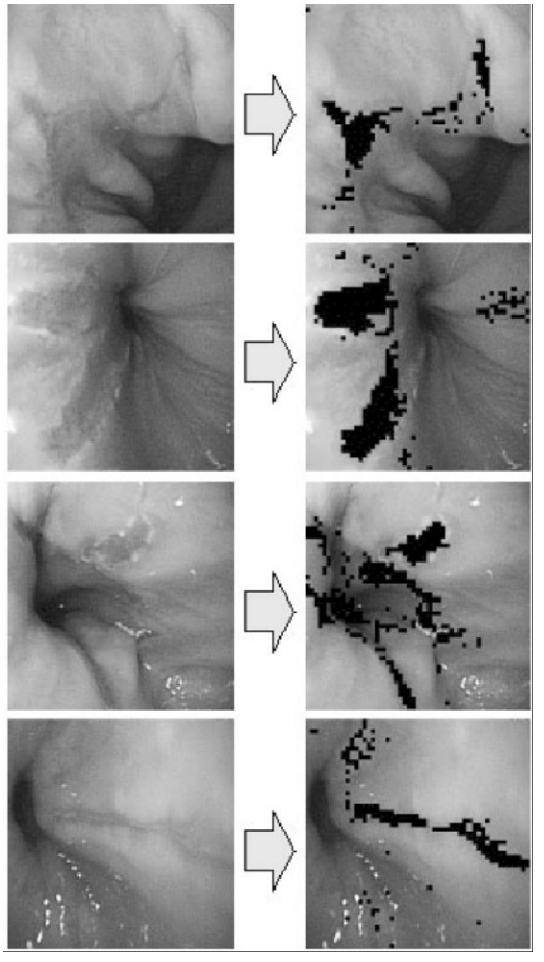

Fig. 4 Validated original and resultant images

5. Conclusions

Information on the color and textural parameters of endoscopy derived images were collected and examined in this study to detect possible esophageal abnormalities, such as erosion or ulcer, that in ordinary practice might be missed. Subsequently, an algorithm for distinguishing abnormalities from normality's within the images was developed by applying the BPN (Back Propagation Network).

With the developed algorithm, the success rates for detection by the difference in the numbers of the hidden-layer neurons in the BPN were investigated. As the result, it was possible to obtain learning parameters which enable one to distinguish normality's from abnormalities. In addition, the boundary values regarded as a criterion for detection could be optimized from the 7th polynomial expression thereby indicating the success rates by the boundary values. Especially important in this study was the ability to detect esophageal erosions and/or ulcers which are key criteria for the diagnosis of esophagitis. The success rate for detection was equal to 97.91% during the calibration phase using ten images and the mean success rate established at 96.83% during validation. And almost 20% of the abnormal parts have been identified as normal. However, the failure rate means that abnormal images are not normal, but the abnormal locals are normal. Therefore, this failure rate can accept in the application.

The primary cause of error in diagnosing esophagitis may well be that it is not possible to accurately quantify data from a physician's subjective interpretation. The incidence of human error, however, may be reduced by quantifying data collected from the opinions of several examiners, but as this study demonstrates, the success rate of detection of esophagitis can be im-

proved by applying the described algorithm to a real-time examination for esophagitis.

Acknowledgements

This study was supported by a grant from the Korea Health 21 R&D Project, Ministry of Health & Welfare, Republic of Korea. (02-PJ3-PG6-EV06-0002); Corresponding author : D.W. Lee.

References

Karkanis, S. A., Iakovidis, D. K., Maroulis, D. E., Magoulas, G. D. and Theofanous, N., 2000, "Tumor recognition in endoscopic video images using Artificial Neural Network Architectures," *26th EUROMICRO Conference, Medical Informatics, Mastricht*, pp. 423～429.

Krishnan, S. M. and Zheng, M. M., 2002, "Data Fusion Application for Computer Assisted Clinical Endoscopic Image Analysis," *Proceeding of the 2002 ieee Canadian Conference on Electri cal & Computer Engineering*, pp. 1116～1119.

Krishnan, S. M. and Yang, X., 1998, "Intestinal Abnomality Detection From Endoscopic Images," *Proceedings of the 20rd Annual International Conference of the IEEE Engineering*, Vol. 20, No. 2, pp. 895～898.

Na, Y. H., Chang, M. K., Yoo, J. K. and Song, S. R., 1994, "Growth Rate of Esophagitis In Gastro Esophageal Disease," *The Korean Journal of Gastrointestinal Endoscopy*, Vol. 2, pp. 145～150.

Nguyen, D. and Widrow, B., 2001, "Improving the Learning Speed of Two-Layer Neural Networks by Choosing Initial Values of the Adaptive Weights," *IEEE Int. Joint Conf. on Neural Networks*, Vol. 3, pp. 21～26.

Parker, J. R., 1997, "Algorithms for Image Processing and Computer Vision," *Wiley*, pp. 150～175.

Paul Fockens, 2002, "Future Developments in Endoscopic Imaging," *Best Practice & Research Clinical Gastroenterology*, Vol. 16, No. 6, pp. 999～1012.

Seo, K. W., Lee, C. W., Kim, W., Lee, S. Y. and Lee, D. W., 2004, "Image Discriminal Analysis for Detecting a Esophagitis," *Journal of the Korea Society of Medical and Biological Engineering*, Vol. 25, No. 6, pp. 545～550.

Tjoa, M. P. and Krishnan, S. M., 2001, "Segmentation of Clinical Endoscopic Image Based on Homogeneity and Hue," *Proceedings of the 23rd Annual EMBS International Conference*, Vol. 3, pp. 2665～2668.

Wang, P. and Krishnan, S. M., 2001, "Classification of Endoscopic Images Based On Texture and Neural Network," *Proceedings of the 23rd Annual EMBS International Conference*, pp. 3691～3695.

Yoon, Y. H., Kang, Y. W., Ahn, H. H. and Park, S. K., 2001, "The Change of Gastro Esophageal Reflux Disease in Resent," *The Korean Journal of Gastrointestinal Endoscopy*, Vol. 23, pp. 144～148.

Zheng, M. M. and Krishnan, S. M., 2001, "Decision Support by Fusion In Endoscopic Diagnosis," *Seventh Australian and New Zealand Intelligent Information Systems Confercence*, pp. 107～110.